THE SYNTHESIS AND CHARACTERIZATION OF GROUP ONE METAL TITANATES AND THEIR APPLICATION IN PHOTOCATALYSIS

by

NUR RUZAINA BINTI ABDUL RAHMAN

Thesis submitted in fulfillment of the requirements
for the degree of
Master of Science

April 2019

ACKNOWLEDGEMENT

Bismillah hir rahman nir Rahim all praise to ALLAH s.w.t and salutation upon the Prophet Muhammad s.a.w, and his companions. *Alhamdulillah*, finally I managed to complete my master's research successfully with full of patience and contentment. First and foremost, I would like to thank my supervisor, Prof. Dr. Farook Adam for his guidance, encouragement, understanding and freedom in research as well as in discussion. The most wonderful things about him was his scientific knowledge and wisdom in solving problem. May Allah s.w.t bless him and his entire family.

I would also like to thank my co-supervisors, Dr. Muhammad Anwar Mohamed Iqbal and Assoc. Prof. Dr. Ng Eng Poh for their support, advice and valuable comments on this thesis. Special thanks to Dr. Lingeswarran for his help, council and criticism for improvement. I would also like to express my gratitude to Prof. Rohana, Prof. Srimala and Dr. Lee Hooi Ling for their valuable suggestion and for giving access to their laboratory and research facilities. Without their precious support it would not be possible to complete this research.

I would like to thank all staffs of the School of Chemical Science, USM, School of Physics, School of Archeology and Research Center SERT in the Engineering Campus USM for their help and commitment. I would like to acknowledge the financial support provided by the University Science Malaysia in the form of Research University Grant Scheme (1001/PKIMIA/811269 and 203/PKIMIA/6720009). I also wish to express gratitude to my fellow colleagues Ms. Fatehah, Ms. Umie Fatihah, Mdm. Fatimah, Ms. Farah Waheed, Mdm. Vicky Inderan, Mdm. Risha, Ms. Logeishwarry, Ms. Hanisah, Ms. Amira, Mr. Tan, Mr. Muhammad Faizal, Mr. Usman and Mr. Ismail with whom I enjoyed working during my research.

My deepest thanks go toward my parents Mr. Abdul Rahman Muhammad and Mdm. Hameedah A. Ibrahim for being my backbone. Their endless prayer, support and encouragement gave me strength throughout my journey. May Allah s.w.t bless them with Jannah. Special thanks to my siblings Muhammad Akashah, Masyitah and Ammar Yasir for your love, care and endless support. Not forgetting, my grandparents on maternal side Mr. Ibrahim and Mdm. Subaidah for their love and affection to overcome all the difficulties. On my paternal side, Mr. Muhammmad and Mdm. Raheemah for their encouragement. And to my fiancé, thank you for your attention, moral support and care, may Allah s.w.t make everything easy for us. Lastly, a big thank you to all who supported me throughout my work and whose names I might have missed out here. May Allah s.w.t reward you with peace and happiness. *Wassalamualaikum warahmatullahi wabarakatuh.*

TABLE OF CONTENTS

CHAPTER 3 - EXPERIMENTAL

CHAPTER 4 - CHARACTERIZATION AND MECHANISM OF GROUP ONE METAL TITANATE FORMATION

LIST OF TABLES

Page

LIST OF FIGURES

Page

LIST OF SCHEMES

Page

LIST OF APPENDICES

LIST OF ABBREVIATIONS AND SYMBOLS

$\bullet O_2^-$	Superoxide radical
•OH	Hydroxyl radical
1 D	One dimensional
A	Anatase
AC	Activated Carbon
B	Brookite
IC	Ion chromatography
BET	Brunauer-Emmett-Teller
BJH	Barett Joyner and Halenda
CB	Conductive Band
CTAB	Cetyl trimethylammonium bromide
DFT	Density function theory
DRS	Diffuse Reflectance spectroscopy
e^-	Electron
HTA	Hydroxyterephthalic acid
ICP Ms	Inductively coupled plasma mass spectrometry
ICP OES	Inductively coupled plasma atomic emission spectroscopy
IUPAC	International Union of Pure and Chemistry
K_L	Langmuir constant

K_{LH}	Langmuir Hinshelwood constant
K_F	Freundlish constant
KOH	Potassium Hydroxide
LED	Light Emitting Diode
LiOH	Lithium Hydroxide
MB	Methylene Blue
MO	Methylene Orange
NAD	Nitrogen adsorption desorption
NaOH	Sodium Hydroxide
NBs	Nanobiscuits
NPs	Nanoparticles
NRs	Nanoribbons
NTs	Nanotubes
NWs	Nanowires
O_2	Oxygen
OH^-	Hydroxyl ion
R	Rutile
TA	Terephthalic acid
TiO_2	Titanium dioxide
UV	Ultraviolet
VB	Valence band

SINTESIS DAN PERINCIAN TITANAT LOGAM KUMPULAN SATU DAN APLIKASI DALAM FOTOPEMANGKINAN

ABSTRAK

Titanat logam kumpulan satu telah disintesis melalui kaedah hidrotermal menggunakan hidroksida kumpulan logam satu seperti LiOH, NaOH, KOH dan CsOH. Keputusan menunjukkan pembentukan nanobahan seperti Li-$TiO_2$200^oC/12h nanobiskut (NBs), Na-$TiO_2$200^oC/12h nanoriben (NRs), K-$TiO_2$200^oC/12h nanowayar (NWs) dan Cs-$TiO_2$200^oC/12h nanobebola (NSs). Corak XRD Li-$TiO_2$200^oC/12h, K-$TiO_2$200^oC/12h dan Cs-$TiO_2$200^oC/12h menunjukkan kehadiran fasa anatas dominan di (101) kecuali Na-$TiO_2$200^oC/12h. Ini disebabkan ion Na^+ dalam kekisi anatas yang mengherotkan fasa anatas kepada fasa natrium titanat. Ini sepadan dengan keputusan ICP-OES yang menunjukkan peratus nisbah molar Na/Ti ialah 0.161 lebih tinggi berbanding dengan K/Ti ialah 0.157 dan Li/Ti ialah 0.046. Tambahan pula, peak dekonvulasi Na 2p pada isyarat XPS 1071.3 eV and 1070.3 eV sesuai dengan kehadiran ikatan Na-O-Ti. Di samping itu, pengawalan parameter seperti suhu hidroterma dan tempoh hydroterma semasa sintesis, menghasilkan perubahan dalam morfologi serta saiz zarah titanat. Analisis Dr-UV / Vis menunjukkan tenaga jurang band untuk Li-$TiO_2$200^oC/12h, Na-$TiO_2$200^oC/12h, K-$TiO_2$200^oC/12 dan Cs-$TiO_2$200^oC/12h masing-masing ialah 3.12, 3.05, 3.07 dan 3.17 eV. Kawasan permukaan sampel ialah 32.0, 120.0, 155.0 dan 24.3 m^2g^{-1} untuk Li-$TiO_2$200^oC/12h, Na-$TiO_2$200^oC/12h, K-$TiO_2$200^oC/12h dan Cs-$TiO_2$200^oC/12h masing-masing. Kajian fotopemangkin menunjukkan bahawa Li-$TiO_2$200^oC/12h mempamerkan kecekapan fotopemangkin yang tinggi serta mendegradasikan MB lebih baik berbanding Degussa P25 dan anatase TiO_2. Kepekatan anion sulfat apabila Li-$TiO_2$200

°C/12h digunakan, didapati meningkat dari 2.30 hingga 6.40 mg L^{-1}. Ini adalah 52.8% kandungan sulfur dari MB. Sedangkan untuk Degussa p25, kepekatan ion sulfat meningkat dari 1.56 hingga 6.21 mg L^{-1} yang berkorelasi kepada 51.3% daripada kandungan sulfur dari larutan MB selepas sejumlah 4 jam di bawah sinaran suria. Sementara itu, K-$TiO_2$200^{o}C/12h, Na-$TiO_2$200^{o}C/12h dan Cs-$TiO_2$200^{o}C/12h menunjukkan sifat penjerapan yang dominan. Kajian mendalam menggunakan XPS, menunjukkan persamaan antara titanat alkali seperti Li-$TiO_2$200^{o}C/12h, Na-$TiO_2$200^{o}C/12h, K-$TiO_2$200^{o}C/12h dan Cs-$TiO_2$200^{o}C/12h mempunyai tapak kecacatan Ti^{3+} yang juga dikenali sebagai tapak kekosongan oksigen. Pembentukan Ti^{3+} atau tapak kekosongan oksigen berkemungkinan disebabkan saiz ion logam dan polarisasi logam (e.g. Li^+, Na^+, K^+ dan Cs^+) masing-masing, yang kemudiannya mempengaruhi jenis doping (e.g Interstisial atau penukarganti). Kehadiran kekosongan oksigen atau Ti^{3+} membantu mengurangkan nisbah rekombinasi lubang dan elektron serta meningkatkan aktiviti fotopemangkinan. Walau bagaimanapun, didapati bahawa K-$TiO_2$200^{o}C/12h mempunyai keadaan Ti^{3+} berlebihan yang berkemungkinan bertindak sebagai pusat rekombinasi untuk lubang dan elektron seperti ditunjukkan dalam analisis PL. Oleh itu, prestasi photocatalytic tidak hanya berasaskan analisis PL tetapi dengan justifikasi lebih lanjut melalui kajian mineralisasi. Li-$TiO_2$200^{o}C/12h didapati menjadi pemangkin terbaik kerana ia mempunyai sifat penjerapan dan photocatalytic. Li-$TiO_2$200^{o}C/12h telah digunakan semula sehingga empat kitaran tanpa penurunan ketara dalam aktiviti pemangkin.

THE SYNTHESIS AND CHACTERIZATION OF GROUP ONE METAL TITANATES AND THEIR APPLICATION IN PHOTOCATALYSIS

ABSTRACT

Group one metal titanates has been synthesized via hydrothermal method using group one metal hydroxides. The results show the formation of nanomaterials such as Li-$TiO_2$200^oC/12h nanobiscuits (NBs), Na-$TiO_2$200^oC/12h nanoribbons (NRs), K-$TiO_2$200^oC/12h nanowires (NWs) and Cs-$TiO_2$200^oC/12h nanospheres (NSs). The XRD patterns of Li-$TiO_2$200^oC/12h, K-$TiO_2$200^oC/12h and Cs-$TiO_2$200^oC/12h showed the presence of the dominant anatase phase at (101) except for Na-$TiO_2$200^oC/12h. This was due to the Na^+ ion within the anatase lattice resulting in the distortion of the anatase phases and formation of the sodium titanate phases. This was in agreement with the ICP-OES result which showed the molar ratio of Na/Ti was 0.161 which was higher than K/Ti(0.157) and Li/Ti(0.046) respectively. In addition, the deconvolution of the Na 2p XPS signal showed the presence of peaks at 1071.3 eV and 1070.3 eV corresponding to the Na-O-Ti species. Besides that, controlling the hydrothermal temperature and the duration of synthesis, resulted in changes in the morphology as well as the particle size of the titanates. The Dr-UV/Vis analysis indicated the band gap energy of Li-$TiO_2$200^oC/12h, Na-$TiO_2$200^oC/12h, K-$TiO_2$200^oC/12 and Cs-$TiO_2$200^oC/12h to be 3.12, 3.05, 3.07 and 3.17 eV respectively. The surface area of the samples was calculated to be 32.0, 120.0, 155.0 and 24.3m^2g^{-1} for Li-$TiO_2$200^oC/12h, Na-$TiO_2$200^oC/12h, K-$TiO_2$200^oC/12h and Cs-$TiO_2$200^oC/12h respectively. Photocatalytic study revealed that Li-$TiO_2$200^oC/12h exhibited enhanced photocatalytic efficiency and mineralized MB better compared to Degussa P25 and anatase TiO_2. The concentration of sulphate anion when Li-$TiO_2$200°C/12h was used,

was found to increase from 2.30 to 6.40 mg L^{-1}. Whereas for Degussa P25, the concentration of sulphate ion increased from 1.56 to 6.21 mg L^{-1} after 4 h under solar irradiation. Meanwhile, K-$TiO_2$200^oC/12h, Na-$TiO_2$200^oC/12 and Cs-$TiO_2$200^oC/12h showed dominant adsorption properties. In-depth characterization using XPS, showed similarities between thee group one metal titanates. Li-$TiO_2$200^oC/12h, Na-$TiO_2$200^oC/12h, K-$TiO_2$200^oC/12h and Cs-$TiO_2$200^oC/12h have Ti^{3+} moieties, also known as oxygen vacancy sites. The formation of Ti^{3+} moieties or oxygen vacancies was induced by the size of the metal ions and their polarizability (i.e. Li^+, Na^+, K^+ and Cs^+), which later influenced the types of doping (i.e. interstitial or substitutional). The presence of Ti^{3+} species help to reduce the electron hole recombination ratio as well as increased the photocatalytic activity. However, it was found that K-$TiO_2$200^oC/12h had excessive Ti^{3+} species which probably acted as a electrons/hole recombination center as shown in the PL analysis. Therefore, the photocatalytic performance was based on the PL analysis with further justification through mineralization studies. Li-$TiO_2$200^oC/12h was found to be the best catalyst since it had both adsorption and photocatalytic properties. The Li-$TiO_2$200^oC/12h was reused up to four cycles without much deterioration in the catalytic activity.

CHAPTER 1

INTRODUCTION

1.1 Background study

The increased population growth in the world has let to toxic waste discharges especially dyes resulting in severe contamination of major water bodies. Thus, sustainable water treatment that meets the global needs is paramount. The application of TiO_2 as a viable photocatalyst is an interesting alternative for environmental remediation especially in waste water treatment (Nakata and Fujishima, 2012). This is due to the photo-stability, non-toxicity and the capacity of TiO_2 to mineralize organic and inorganic materials under UV irradiation (Kumar and Devi, 2011).

Previously, adsorption process utilizing activated carbon (AC) had been widely used in waste water treatment for the removal of pollutants. The presence of a variety of pore sizes, volume and specific surface area of AC promises enhanced adsorption capacity for adsorbates with exceptionally large molecular weight (Pietrzak et al., 2014). However, once the adsorbent has been saturated with the adsorbate, significant desorption might occur. This would eventually release the pollutants back into the water bodies. Therefore, the adsorption process could be improved remarkably by mineralizing the pollutants. Hence, it would be interesting to synthesize materials which possess dual functionalities for adsorbing and thence, mineralizing the organic molecules.

In order to achieve this target, TiO_2 has been modified into one-dimensional 1D nanostructures. 1D TiO_2 nanostructures proved to have properties such as high aspect ratio structure, chemical stability, large specific surface area, excellent electronic or ionic charge transfer, and a specific interface effect which enhance the

application (Tian et al., 2014). Therefore 1D TiO_2 nanomaterials such as nanotubes, nanowires, nanofibers, nanoribbons, nanobelts has been designed and synthesized by controlling size and morphology using alkaline hydrothermal method (Tian et al., 2014 and Kordás et al., 2015).

Alkaline hydrothermal synthesis was introduced by Kasuga in 1998 and is highly recommended for the fabrication of 1D titanate nanomaterials due to its simplicity and feasibility to handle (Liu et al., 2012). Tomiha et al. (2002) observed various titanate morphologies when different alkali metal hydroxides (LiOH, NaOH and KOH) were used in the hydrothermal synthesis. In addition, Song et al. (2007) had successfully prepared Li_2TiO_3 snowflakes and $Na_2Ti_3O_7$ and $K_2Ti_8O_{17}$ nanorods where these alkali titanates had higher photocatalytic activities compared to Degussa P25 in the degradation of chloroform under UV light irradiation. A review has been carried out on the adsorption and photocatalytic of each group one metal titanates in Chapter 3.

1.2 Problem statement

Research in photocatalysis for the last two decades mainly concentrated on designing 1D group one metal titanates nanomaterials with high photonic efficient catalyst, without understanding the surface phenomena of the catalyst and the targeted application. Therefore, in this thesis the mechanism of formation of the group one metal titanates are discussed using XPS elemental analysis.

The application of titanium dioxide in photocatalysis reaction is well known. However, there exists some problems regarding the efficiency of the catalytic reaction in real waste water treatment. Where the photocatalytic process itself is not comprehensive to treat thousands of liter or mega liter of water per day. The

combination of both processes, i.e. adsorption and photocatalysis, will compensate each other to overcome this problem.

In addition, in real practical application the adsorbed pollutant might not be completely mineralized into carbon dioxide and water in a short period of time. Therefore, we required catalyst that can be generated back under sunlight without any other additional treatment.

1.3 Research objectives

This thesis reports the designing of a novel group one metal titanate nanocatalyst for the mineralization of methylene blue, MB. The objectives of the research are:

1. To design group one metal titanates with nanostructures by controlling the hydrothermal temperature, time and different group one metal hydroxyl solution (i.e. lithium, sodium, potassium and caesium).
2. To study the physical properties and mechanism formation of Ti^{3+} or oxygen vacancy.
3. To study the adsorption and photocatalytic potential of the group one metal titanates in the mineralization of MB.

1.4 Scope of study

This study consists of three major parts which was separated in chapter 4 and 5. The first parts discussed on the synthesis of group one metal titanates nanomaterials using group one metal hydroxyl solution (e.g LiOH, NaOH, KOH and CsOH) by controlling the hydrothermal duration and hydrothermal temperature. This synthesized group one metal titanates where then characterized using FTIR, TEM, XRD, NAD and applied in photocatalytic degradation of MB dye to determine the highest photo active group one metal titanates.

The second parts consist of in depth characterization of the highest photo active group one metal titanates synthesized at 200^{o}C/12h using DRS, HR-TEM, PL, ICP-OES and XPS to determine the factor contributed to the photocatalytic efficiency of group one metal titanates as well as to understand the formation of Ti^{3+} moieties. This first and second part were discussed in chapter 4.

The third part consist of detailed study on the adsorption, thermodynamic, photocatalytic, mineralization and reusability of high photo active group one metal titanates synthesized at 200^{o}C/12h. Several parameters have been optimized during the adsorption studies such as the effect of initial MB concentration (10 – 100 mg/L), mass of dosage (0.05 – 2.0 g), effect of contact time (0 to 120 min) and effect of temperature (298, 318, 328 K). Thermodynamic study conducted to determine the types of adsorption of each respective group one metal titanates (e.g physisorption or chemisorption) using Gibbs free energy (ΔG) and Van't Hoff linear equation.

Photocatalysis study was further conducted after the adsorption process under solar irradiation at intensity $\approx$ 800 Wm^{-2}. Here a comparison studies has been conducted between each respective group one metal titanates with commercially available degussa P25 and anatase, TiO_2. Several other parameters such as the kinetic rate of photocatalytic reaction, the radical scavenging effect and rate of hydroxyl radical production has been carried out to determine the efficiency of MB degradation and the dominant radicals that contribute to the photocatalytic degradation of MB. Mineralization studies using IC has been conducted to prove the degradation of MB molecules into CO_2, water, small fragment and anions. Lastly, reusability test was also conducted to determine the efficiency of the catalyst under sunlight.

CHAPTER 2

LITERATURE REVIEW

2.1 Adsorption - Theory and application.

Adsorption is a surface process whereby the adsorbate (e.g. gas or liquid) molecules or ions adhere on the adsorbent (e.g. solid) surface. It is different from the absorption process in which the adsorbate molecules penetrate into the voids of the adsorbent. In general, both processes are known as sorption. Adsorption was categorized into chemical adsorption (or chemisorption) and physical adsorption (or physisorption), depending on the types of bonding involved in the process. In chemisorption, adsorbates are strongly bonded to the surface adsorbent by sharing or exchanging electrons and is more favorable under endothermic condition. In physisorption, adsorbates are weakly bonded to the surface of the adsorbent by van der Waals force or electrostatic attraction (Dabrowski,. 2001). The adsorption mechanism can be determined by fitting the adsorption data into suitable adsorption modals and further confirmed through thermodynamic studies at different temperature.

Adsorption model has been categorized into an adsorption isotherm model and adsorption kinetic model. Over the years, the most commonly used adsorption isotherm models are Langmuir, Freundlich, Temkin and Dubinin-Radushkevich (Tan and Hameed, 2017). Meanwhile, the prevalent adsorption kinetic model utilized was the pseudo-first order, pseudo-second order and intraparticle diffusion model (Shah et al., 2015). Based on the adsorption isotherm data obtained, the changes in thermodynamic parameters such as Gibbs free energy (ΔG), enthalpy (ΔH) and entropy (ΔS) of the system can be determined to confirm whether the adsorption process is

spontaneous or non-spontaneous, exothermic or endothermic and whether the adsorption process is favorable or not favorable (Shah et al., 2014).

Adsorption isotherm obtained from N_2 adsorption desorption analysis (NAD) explains the surface properties and the porous network of the respective adsorbent. The NAD process charts the relationship between the amount of gas (usually N_2) adsorbed and the pressure applied at constant temperature. According to International Union of Pure and Applied Chemistry (IUPAC) there are six (I to IV) types of adsorption isotherms. These isotherms (I to V) were proposed by Brunauer, Emmett and Teller (BET) (Donohue and Aranovich, 1998). Each types of adsorption isotherm has specific sigmoid graph with/without hysteresis loop which can be used to explain the affinity of the adsorption process and the porous networks of the adsorbent.

The adsorption process is mainly applied in waste water treatment using activated carbon (AC) as the adsorbent due to its high surface area and multiple pore sizes. However, secondary pollution resulted due to factors such as inappropriate disposal of the AC (Zhang et al., 2007 and Ai et al., 2010), metal ion released into the treated water without catalyst support (Hu et al., 1999) and also due to the desorption process. Desorption is the reverse process of adsorption whereby the removal of the accumulated adsorbate molecules will be released back into the bulk solution which might cause secondary pollution (Zhang et al., 2005). This problem can be compensated through photocatalysts process, whereby the adsorb material will be degraded under solar irradiation into carbon dioxide and water. The synergistic effect offered by the adsorption and photocatalysis process promises a better waste water treatment system in the future.

2.2 Photocatalysis – Theory and application

Photo-catalysis is a process that uses light to activate catalysts for chemical reactions. This process mimics the natural photosynthesis process that occurs in plants. In both processes, light is converted to chemical energy. Even the leaves in plants has been taken as a good example in designing material for hydrogen generation by understanding the leave structure (Zhou et al., 2010). Photocatalysis is used in a variety of practical applications ranging from environmental remediation, solar fuel production, free energy generation and pharmaceutical application.

The basic mechanism of photocatalysis of semiconductors e.g. TiO_2 is initiated by the illumination of UV radiation from sunlight or artificial light and create photo induced charges (e.g. electron and holes). The electron and hole pairs can only be created if the energy of light falling on the photocatalyst is equal or greater than the band gap energy of the catalyst. When the electrons excite from the valence band (VB) to the conductive band (CB), holes will be created. The holes will be oxidized to hydroxyl radicals (•OH) upon interaction with hydroxyl ion ($^-$OH) from the moisture in the air. The electron in the CB will be scavenged by the oxygen molecules (O_2) from the environment and reduced to superoxide radicals ($\bullet O_2^-$). The hydroxyl radical has high oxidizing power and are capable to mineralize organic and inorganic compounds, including microbes, ideally to carbon dioxide and water (Ibhadon et al., 2013). The photocatalysis process is shown in Fig. 2.1.

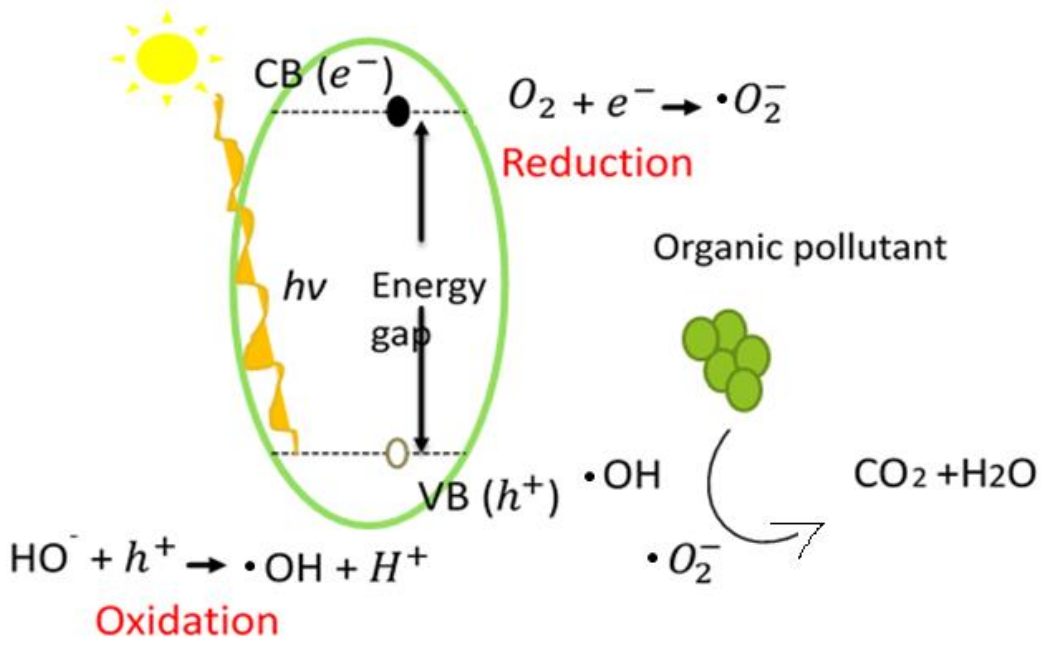

Figure 2.1 The general mechanism of photocatalysis showing the generation of electron and hole pairs due to the ejection of electrons from the valence band (VB) to the conducting band (CB).

During the photocatalysis reaction, the generated electrons and holes can recombine and release the absorbed light energy as heat as shown in Fig. 2.2. The recombination rate of the electron and hole pairs is one of the factors that determine the efficiency of the photocatalysts. Slower rate of recombination is preferred so that more radicals will be generated to degrade pollutants.

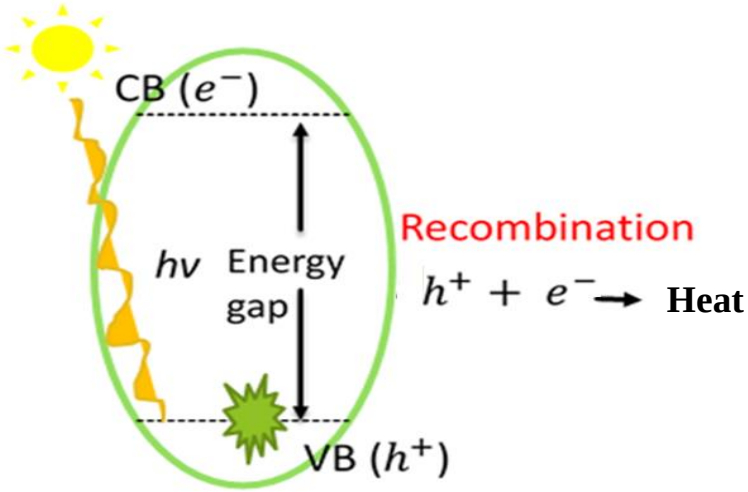

Figure 2.2 Shows the recombination process of the electron and hole charges releasing heat energy.

There are two main photo-induce redox reactions that occur on the TiO_2 surface once irradiated with UV light. Those are photo-oxidation in the VB and photo-reduction on CB. If the targeted application is the oxidation of complex organic molecules (the pollutants), then the hole potential at the VB is very critical. Same goes to the photo-reduction reaction. For example, in hydrogen generation and carbon dioxide reduction applications. If the targeted application is reduction of water to form hydrogen gas then the generation of multiple electron transfer to the CB is very important (Park et al., 2016).

2.2.1 Light Source for Photocatalysis

The development of photo-catalysis technology for indoor application using light sources such as xenon lamp, halogen lamp, LED lamp and mercury lamp have resulted in many publications as reported in Table 2.1. The source of light plays a vital role in photo-catalytic activity. Based on Table 2.1, sunlight shows the best

photocatalytic activity as compared to artificial light. The production of photo-induced charges and the excitation of electrons to the higher energy levels depend on the energy supplied by the light source. The energy must be equal to or higher than the band gap energy of the particular catalyst. Artificial light is beneficial for indoor application however there are few specification that need to be consider before using the light. Those specification are the spectrum, intensity, spread, consistency, format, fitting and type, longevity and reliability including source of light materials and the cost of artificial light must be considered.

Though effective, these lamps faced some drawbacks. Sunlight is a sustainable and green source of light provided by nature to us. The total energy power received by the earth surface from the sun at the zenith is about 1050 W/m^2 depending on the distance between the earth and the sun. Sunlight is a portion of energy from sun in the form of light which comprise of electromagnetic radiation. The total electromagnetic radiation consumed by the earth's residence is only 52 to 55% of infrared light (above 700 nm), 42 to 43% of visible light (400 to 700 nm) and 3 to 5% of ultraviolet light (below 400 nm) (Chowdhury et al., 2017, and Chowdhury P., 2012). The earth's atmosphere filters almost 70% of the shorter wavelength of UV rays before living things get to use the energy to avoid hazardous high energy UV radiation. Several devices have been invented to measure the sunlight radiation such as sunshine recorder, pyranometer or radiometer in watt per square meter (W/m^2) as reported by (Borges et al., 2016).

The use of solar power in technology nowadays is numerous. In Germany, the evolution of photovoltaic (PV) technology enabled the efficient conversion of light energy from the sun to electrical energy through electron flow. The electrical energy generated are sufficient for the operation of electronic devices (Wirth, 2015). Besides

that, in 2005 the terminal building of Chubu international airport in Japan was completely installed with 20,000 cm^3 self-cleaning exterior glass. While in Belgium, 10,000 m^2 concrete paving blocks coated with TiO_2 material has been installed to overcome air pollution (Boonen and Beeldens, 2005). In 2006, Katzman studied the cost and effectiveness of coating the building with TiO_2 catalyst to overcome air pollution (Katzman, 2006). He found that even though the major drawback of utilizing photocatalytic building materials are the cost and the limited commercial availability in the United State, it can still be considered due to longevity to maintain self-clean and reduce the cost for maintenance. For example, TPX 85 is a transparent coating for self-cleaning concrete surface from Green Millennium company in US can last for at least ten years and has been utilized in Japan. This proved that sunlight is compatible for industrial.

Table 2.1 The properties of light and the photocatalytic efficiency in overcoming various organic and inorganic pollutant.

No	Types of photo-catalyst	Pollutant	Source of light	Results	Ref
1	-Degussa p25 -C-doped Titania -Fe-doped Titania	-Amoxicillin (AMO) -β-Lactam antibiotic	-Mercury UV lamp (365 nm, 15W, 0.5mW/cm^2) -Fluorescent lamp (33-640 nm, 15W, 0.6 mW/cm^2) -Natural Solar (16 mW/cm^2)	-Doped catalyst efficiency is closed to Degussa P25 under solar radiation. -Degradation of AMO under solar irradiation is three times faster than artificial UV.	(Klauson et al., 2010)
2	-Anatase, TiO2 -Rutile, TiO2 -ZnO	-Real Textile industrial waste	-Mercury UV lamp (125 W) -Natural Solar (11am to 1 pm, Desember 2008 to July 2009)	-Complete removal of waste follows ZnO (solar) > ZnO (artificial) > Anatase (solar) > Rutile (solar) > Anatase (artificial) > Rutile (artificial).	(Hussein, 2012)
3	-Degussa P25	-Humic acid	-UVA lamp different intensity (315 to 400 nm, 10 to 15W) intensity 35, 225 and 435μW/cm^2.	-The removal efficiency of humic acid increase with increase in light intensity and becoming asymptotic.	(Pansamut et al., 2013)

4	-Degussa P25-slurry -Degussa-P25 film	Acetaminophen (N-(4-hydroxyphenyl acetamide)	-Mercury UV lamp (200 to 280 nm, 11W) -Natural sunlight (11 am to 2.30 pm)	-The results show TiO_2 suspension/UV system is more efficient than the TiO_2 / cellulosic fiber mode combined to solar light for the photocatalytic degradation of paracetamol.	(Jallouli et al., 2014)
5	-Riboflavin- titanium dioxide nanotubes (RF-TiO_2 NTs	-Indigo carmine (InC) -Methylene Blue (MB) -Methy-orange (MO)	-Mercury–xenon lamp (150W) with Cut of UV Filter ≥ 400 nm -UV source -Vis source	n/a	(Backes et al., 2014)
6.	-V-Ti/MCM-41	-Propylene photo-epoxidation	-Xenon lamp with filter (18.5mW/cm2) -Mercury uv lamp with different filter in the range 0.1 to 0.8 mW/cm2.	-The propylene oxide formation rates is higher in UV than visible light. -The light utilization with mercury arc lamp is better than xenon lamp.	(Nguyen et al., 2014)

7.	-Copper sulphide nanoparticles (CuS NPs)	-Methylene Blue (MB) -Rhodamine B -Eosin Y (EY) -Congo red (CR)	-Mercury UV lamp, (12W, G8T5 philips) -Visible (160W, Hg vapour lamp) -Solar (Nov-Dis 2016, 11am to 2 pm)	-Dyes degradation under sunlight is more efficient than artificial vis and UV light.	(Ayodhya et al., 2015)
8.	-Zinc oxide (ZnO)	-Reactive Blue dye (RB)	-UV lamp (254 nm, 8W) -Light emitting diod LED lamp (365 nm, 1W)	-UV LED twice times better than traditional UV lamp	(Khademalrasool et al., 2016)
9	-Titanium dioxide TiO_2	-Propanollo (PRO)	-Xenon lamp -Natural sunlight	-PRO removal under solar is 77 % while in visible light is 71 %.	(He et al., 2016)
10	-Silver nanoparticles	-Azo dye	-UV light -Solar light	-The degradation was higher in the UV light source than in the Solar light sources.	(Mariselvam et al., 2016)

n/a = Not available.

2.3 Alkaline Hydrothermal Method

Alkaline hydrothermal is a well-known method to synthesize different morphology of 1D nanoparticles under high pressure, high temperature and high concentration of group one metal hydroxide solution (Kasuga et al., 1998). Fig. 2.3 represent the standard procedure of the alkaline hydrothermal synthesis discovered by Kasuga. Hydrothermal method was carried out using a stainless-steel autoclave with internal Teflon cylinder as shown in Fig. 2.4.

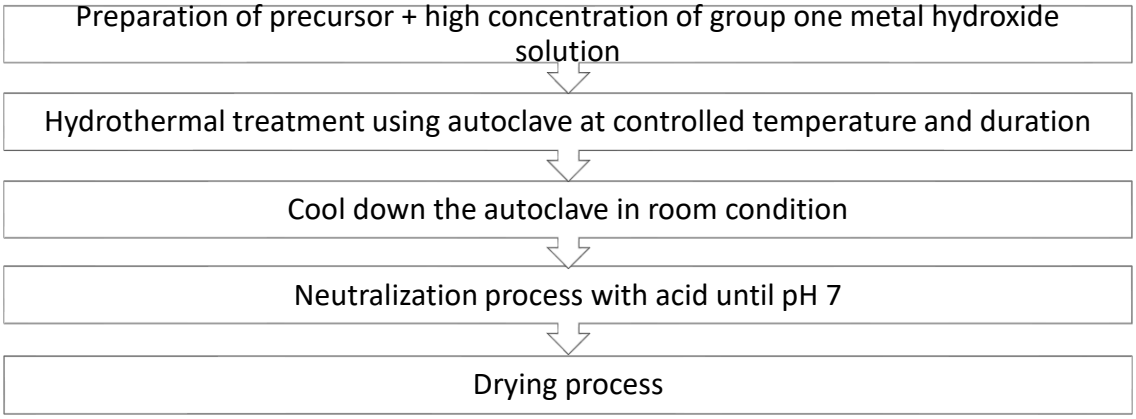

Figure 2.3 The standard procedure of hydrothermal method.

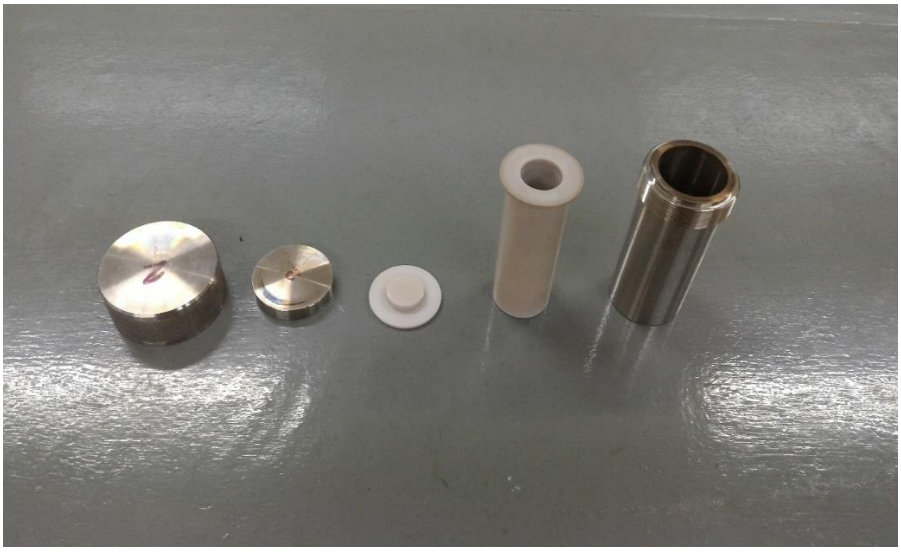

Figure 2.4 Autoclave devices used during the hydrothermal synthesis.

Researchers have modified the standard procedure shown in Fig. 2.3. Some of these modifications includes types of starting precursor, the concentration of acid washing solution types of acid washing solution and addition of calcination treatment was reported in Table 2.2. The significance of these processes is still debatable. Therefore, some literature discussed in detail on the effect of different washing solution by varying the acid concentration (Li et al., 2011), pH (Bem et al., 2012), prolong washing time (Qamar et al., 2006) and also washing with different types of acid solution (Qamar et al., 2006).

Neutralization treatment using different types of acid at different concentration and different condition effect the ion exchange process between group one metal cation such as Na^+ with H^+ ion as been elaborate in Table 2.2. Total removal of cation forming hydrogen titanate (Yu et al., 2007) or titanate alone (Lai et al., 2015) during the acid washing process is possible under extreme conditions as reported by (Lee et al., 2007, Yoshida et al., 2005, Thennarasu et al., 2013 and Nguyen and Bai, 2015). However, the total removal of cation can cause destruction of the nanotube structure (Lee et al., 2007).

Additional of calcination process in the standard hydrothermal synthesis mainly functions to obtain highly crystalline material and also to get rid of any source of surfactant (An'Amt et al., 2014). Many reported pure crystalline anatase and rutile phases under high calcination temperature (Li et al., 2015). However, high calcination temperature might destroy the resulting nanostructures (Tsai and Teng, 2004, Qamar et al., 2006 and Yu et al., 2007). In term of commercial scale production alkaline hydrothermal method is feasible and possible due to 100 % yield production and minor variation in reaction condition will not affect the product quality severely. This process is non-explosive, water based and green process. (Kordás et al., 2015).

Table 2.2 Summarized the modification made on alkaline hydrothermal treatment and the subsequent effect. *DW = Deionized water

No	Types of precursor	Hydrothermal condition	Neutralization & washing until pH 7	Drying	Calcination	Remarks	Ref
1	As-synthesized anatase + 10M NaOH	150 ^{o}C for 48 h -stirring	-DW (Sample A) -HCl and heat at 40 ^{o}C (Sample B)	Freeze dry at 57 ^{o}C	300 ^{o}C to 900 ^{o}C	-Na contain in sample A is higher than sample B due to effect of washing solvent. -Calcination at 900 ^{o}C caused the total destruction of nanostructure.	(Qamar *et* al., 2006)
2	P25 + 10M NaOH	180 ^{o}C (5 to 72 h) -stirring	1.0 M HCl & DW	80 ^{o}C for 24 h	n/a	Mixture of sodium titanate and hydrogen titanate phase..	(Elsanousi et al., 2007)
3	P25 + 10M NaOH	70 ^{o}C to 150 ^{o}C for 48 h	DW + dipped in 0.1 M HCL solution for 1 H	Room temperature	300 ^{o}C to 600 ^{o}C in air for 1 h	Tubular structure collapse when annealing at 600 ^{o}C (xrd convert to anatase phase)	(Seo et al., 2008)

4	Metatitanic acid + 10M NaOH	160 ^{o}C for 12 h	HCl different concentration (0.001 M, 0.01 M and 0.1 M) for several times	80 ^{o}C for 24h in air	n/a	Different con. of HCl control the amount of Na.	(Li et al., 2011)
5	As-synthesized anatase (TTIP) under acidic condition	200 ^{o}C and (6/12/24/36 h)	Deionized water (DW)	80 ^{o}C for 24 h	n/a	Without present of strong group one metal hydroxide solution, the nanostructure formation limited to nanoparticles only.	(Saif et al., 2012)
7	As-synthesized anatase ($TiCl_4$) + 10M NaOH	130 ^{o}C to 220 ^{o}C (12 to72 h)	DW	Room temperature	n/a	Addition of triethanolamine (TEA) significantly reduce the formation time of the titanate nanotube from 24 to 6 h at 180 ^{o}C.	(Ylhäinen et al., 2012)

8	Anatase + 10 M NaOH + 10% TEA (surfactance)	180 ^{o}C (1/6/12 and 24 h)	0.1 M HCl +DW	60 ^{o}C for 3 h	350 ^{o}C for 3 h	1D titanate nanotube formed in 6 h with surfactant.	(An'Amt et al., 2014)
9	Anatase + 10 M NaOH	150 ^{o}C for 24 h	HCl + DW	100 ^{o}C for 24 h	n/a	1D titanate nanotube formed in 9 h without surfactant.	(Lai et al., 2015)
10	Anatase + 10M NaOH	200 ^{o}C and 24 h	1.0 M HCl & deionized water + ethanol	70 ^{o}C for 6h	900 ^{o}C and 1000 ^{o}C for 2h	-Calcination at 900 ^{o}C shows formation of anatase phase with some $Na_2Ti_6O_{13}$. -Calcination at1000 ^{o}C dominant rutile phase with minor $Na_2Ti_6O_{13}$ appear.	(Li et al., 2015)

n/a = not available

2.4 Titanium Dioxide, TiO_2

Titanium dioxide or titania with a chemical formula TiO_2 is a natural occurring oxide of titanium that can be found in ores such as ilmenite and leuxocene. TiO_2 nanoparticles (NPs) can be synthesized via variety of methods such as sol-gel (acid hydrolysis), electrodeposition (metallic coating), hydrothermal (high pressure and temperature), microwave (high-frequency electromagnetic waves), solvothermal (almost identical with hydrothermal), chemical or physical vapour deposition (condensation from vapor state to solid state), direct oxidation (present of oxidant) and sonochemical method (ultrasound)(Chen and Mao, 2007 and Byranvand et al., 2013).

Titanium precursors mainly consists of titanium alkoxides (TTIP, $Ti(OBu)_4$), titanium halides ($TiCl_4$, TiF_4), titanatranes ($N(CH_2CH_2O)_3Ti–O^iPr$), titanium metal and carboxylate derived compound, titanium sulfate and oxysulfate ($Ti(SO_4)_2$, $TiOSO_4$), and Oxobis(2,4-pentanedionato-O,O′)titanium ($TiO(acac)_2$) (Cargnello et al., 2014). In fact TiO_2 NPs has been commercialized, selling at 377 USD kg^{-1} and registered under CAS No. 13463-67-7 with specification and even cheaper than most of titanium precursors including Degussa P25 (selling at 193 USD 250 g^{-1} and CAS No. 13463-67-7). In addition there were research conducted on the dispersion state, aggregation behavior and directly affects towards aquatic organisms using commercial titanium dioxide nanoparticles is safe in natural and synthetic water (Ottofuelling et al., 2011).

In general there were three known crystal forms of titania, i.e. anatase (tetragonal), rutile (tetragonal) and brookite (orthorhombic) as shown in Scheme 2.1 (Ibhadon et al., 2013). Anatase TiO_2 is the most stable form and exhibits high photocatalytic activity compared to rutile and brookite. This is due to its band gap energy of 3.2 eV and small effective mass, which promotes the migration of photo

induced charges and inhibit the recombination of the charges (Zhang *et al.*, 2014). Annealing anatase, TiO_2 at temperatures above 600 to 700 ^oC induces the transformation of anatase to rutile (Hanaor and Sorrell, 2011). Rutile is known as thermodynamically stable crystal phase with direct energy band gap of 3.0 eV. Even though the band gap energy of rutile is smaller than anatase, it is still not efficient in photo-catalysis reaction. In order to increase its photocatalytic ability, rutile TiO_2 is usually mixed with approximately 75% of anatase. This combination is commercially known as Degussa P25. Degussa P25 has higher photo-catalytic activity than anatase due to the synergic effect between anatase and rutile phases (Siah et al., 2016, Mohamed et al., 2014 and Wang et al., 2014). Brookite phase has a band gap energy of 3.3 eV. In addition, its crystal is unstable and is only sparingly discussed in catalytic work. However, the synergistic effect between anatase and brookite is known and shows good photo-reduction of CO_2 into fuels (Zhao et al., 2013).

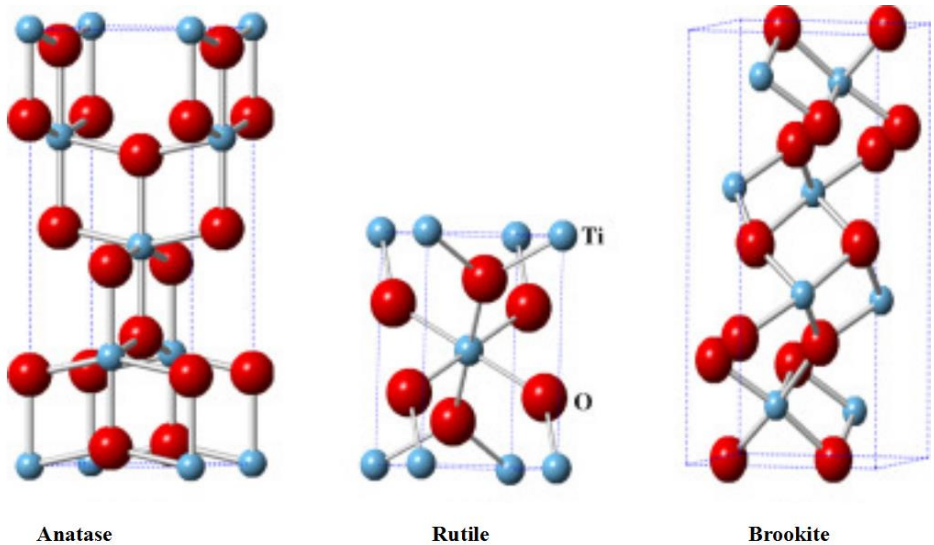

Scheme 2.1 The polycrystal structures of natural occurring titanium dioxide.

Nevertheless, anatase has several drawbacks that limits its use in photo-catalysis reaction. The wide and gap of anatase (3.2 eV) limits its ability to initiate the

photo-induced charges known as electron and holes under visible light. Besides, anatase also has high electron-hole recombination ratio. This recombination causes the absorbed energy to be released as waste in the form of heat. This can be solved by trapping the electrons produced at the vacant position of oxygen, which will result in a decreased number of electron and increase in the number of free holes. The abundance of free holes, increase the chance of interaction with water to form many hydroxyl radicals. This hydroxyl radicals is vital in photocatalysis reaction (Fig. 2.1 and Fig. 2.2).

2.5 Group one metal Titanates Nanostructures.

The synthesis of group one metal titanates nanostructures have been extensively studied because of their unique morphology and novel properties. Generally, a 1D nanostructure is constructed with a high aspect ratio (diameter to length), and at least one of its dimensions should be in the1-100 nm range, no matter whether it is rod-, wire-, belt- or tube shaped (Tian et al., 2014, Chen and Mao, 2007). An ideal nanostructure in photocatalytic application must possess certain criteria such as high specific surface area with many active sites, broad light absorption properties to have the full access to the solar spectrum. It must also have good separation of photo-induced charges for production of more active radicals and finally, if used in a mixture, must contribute to the synergistic effect between two crystal phases for efficient photocatalysis process (Hanaor and Sorrell, 2011) as summarized in Table 2.3.

Table 2.3 The summary of synergistic effect between mixture phases

No	Mixture Phases	Application	Refferences
1.	A & B	Photoreduction of fuel	(Zhao *et al.*, 2013)
2.	A & R	Photocatalysis of phenol	(Mohamed et al., 2014)
3.	A & R & B	Photocatalysis of MB	(Mutuma et al., 2015)
4.	A & B	Photocatalytic H_2 production	(Romero et al., 2015)
5.	A & R & B	Photocatalytic of water pollutant.	(Kaplan et al., 2016)
6.	A & R	Dye sensitized solar cells DSSC's	(Guimarães et al., 2016)
7	A & R	Photocatalysis of phenolic compound	(Siah *et al.*, 2016)
8.	A & R	Photocatalysis of nitrobenzene	(Li *et al.*, 2017)
10.	A & R	Photocatalysis of phenol & formic acid	(Elsellami et al.,2018)

A= Anatase, R= Rutile, B= Brookite.

The 1D nanostructures can be easily synthesized using alkaline hydrothermal method by controlling the hydrothermal temperature and duration. A short review has been done on each group one metal titanates on the synthesis condition (e.g. starting precursor, base solution and hydrothermal condition), physical properties of nanostructures and their common application.

2.5.1 Lithium titanate.

Based from Table 2.4, it can be concluded that the formation of different phases of lithium titanate such as $Li_4Ti_5O_{12}$ and Li_2TiO_3 are mainly used for lithium ion battery. The morphology of lithium titanate reported are lamellar, spherical and cubical crystal with a minimum diameter of 10 nm and maximum diameter of 1.5 μm. The surface area of lithium titanate were less reported. Researchers have obtaining a mixture of phases when lithium titanate was calcined at 500 ^oC (Alias *et al.,* 2009 and Nat, 2013) . However as the calcination temperature and the duration increased the anatase phase start to disappear forming single lithium titanate phase (Nat, 2013). Cheng *et al.,* (2015**)** reported the disappearance of anatase phase after calcination at 750 ^oC. Zhang et al., (2013**)** also reported the disappearance of anatase phase after 10 h of calcination at 500 ^oC.